

PROCEEDINGS OF SPIE

[SPIDigitalLibrary.org/conference-proceedings-of-spie](https://spiedigitallibrary.org/conference-proceedings-of-spie)

The thermal-vacuum and security system of the characterization facility for MAJIS/JUICE VIS-NIR FM and SM detectors

Cisneros-González, Miriam E., Bolsée, David, Van Laeken, Lionel, Pereira, Nuno, Gérard, Pierre, et al.

Miriam E. Cisneros-González, David Bolsée, Lionel Van Laeken, Nuno Pereira, Pierre Gérard, Séverine Robert, Ann Carine Vandaele, Özgür Karatekin, François Poulet, Cydalise Dumesnil, Jean Pierre Dubois, Jérémie Hansotte, Michel Le Du, Laurent Picot, "The thermal-vacuum and security system of the characterization facility for MAJIS/JUICE VIS-NIR FM and SM detectors," Proc. SPIE 11443, Space Telescopes and Instrumentation 2020: Optical, Infrared, and Millimeter Wave, 114437G (13 December 2020); doi: 10.1117/12.2576308

SPIE.

Event: SPIE Astronomical Telescopes + Instrumentation, 2020, Online Only

Thermal-vacuum and security system of the characterization facility for the MAJIS/JUICE VIS-NIR FM and SM detectors

Miriam E. Cisneros-González^a, David Bolsée^b, Lionel Van Laeken^b, Nuno Pereira^b, Pierre Gerard^b, Séverine Robert^{a,b}, Ann C. Vandaele^b, Özgür Karatekin^c, François Poulet^d, Cydalise Dumesnil^d, Jean Pierre Dubois^d, Jérémie Hansotte^d, Michel Le Du^e, and Laurent Picot^e

^aInstitute of Condensed Matter and Nanosciences, Université catholique de Louvain, B-1348 Louvain-la-Neuve, Belgium

^bRoyal Belgian Institute for Space Aeronomy (BIRA-IASB), 1180 Brussels, Belgium

^cRoyal Observatory of Belgium (ROB), 1180 Brussels, Belgium

^dInstitute of Space Astrophysics (IAS), 91440 Bures-sur-Yvette, France

^eNational Centre for Space Studies (CNES), 75001 Paris, France

ABSTRACT

MAJIS is part of the science payload of the JUICE mission to be launched in 2022. BIRA-IASB and ROB contribute to MAJIS with the characterization of the VIS-NIR Flight Model (FM) and Spare Model (SM) detectors, including the design, development, and validation of the setup, as well as the data processing pipeline. The VIS-NIR detectors are thermalized within a temperature range from 125 K to 150 K during their characterization campaigns. Moreover, the temperature of their electronic units must always remain above 120 K to avoid any irreparable damage, and below 160 K for operative conditions. Likewise, to avoid any risk of contamination, the detector should preferably be operated below 10^{-5} mbar of vacuum. To fulfill these requirements, a complete security system was developed; it includes redundant thermal control loops, alarms from every pressure and temperature monitoring devices in use, and a robust semi-automatic control system for the pumping and cryocooling equipment. Moreover, the security system is complemented by the Temperature Ground Support Equipment (TGSE), which provides a LabVIEW user-friendly interface to communicate the status of the detector and the vacuum chamber in real-time. This subsystem was successfully validated in May 2020, before the delivery of the FM detector in June 2020. In this paper, we summarize the design, implementation and validation tests of the security system as well as the thermal and vacuum performances of the facility. We also show the thermal behavior of the detector during acquisitions representative of typical MAJIS observations.

Keywords: JUICE, MAJIS, VIS-NIR detectors, security system, closed cycle cryostat, thermometry, LabVIEW, thermal control

1. INTRODUCTION

MAJIS (Moons And Jupiter Imaging Spectrometer) is part of the science payload of the ESA L-Class mission JUICE (Jupiter ICy Moons Explorer), to be launched in 2022 and arrival at Jupiter in 2030. For at least three years, MAJIS will perform detailed observations of Jupiter and the Galilean satellites. It will focus on the following scientific objectives¹: 1) study of the composition and physical properties of the surfaces of the satellites, 2) characterization of the exospheres of the satellites, 3) study of Jupiter's atmosphere at different levels (including auroras, magnetic footprints and hotspots), 4) spectral characterization of the whole Jovian system (including ring system, dust and small inner moons), and 5) monitoring of particular aspects of the satellites (including Io and Europa torii and Io's volcanic activity).

Further author information:

M.C.: E-mail: miriam.cisneros@uclouvain.be, Telephone: +32 (0)2 373 03 50

D.B.: E-mail: david.bolsee@aeronomie.be, Telephone: +32 (0)2 373 03 51

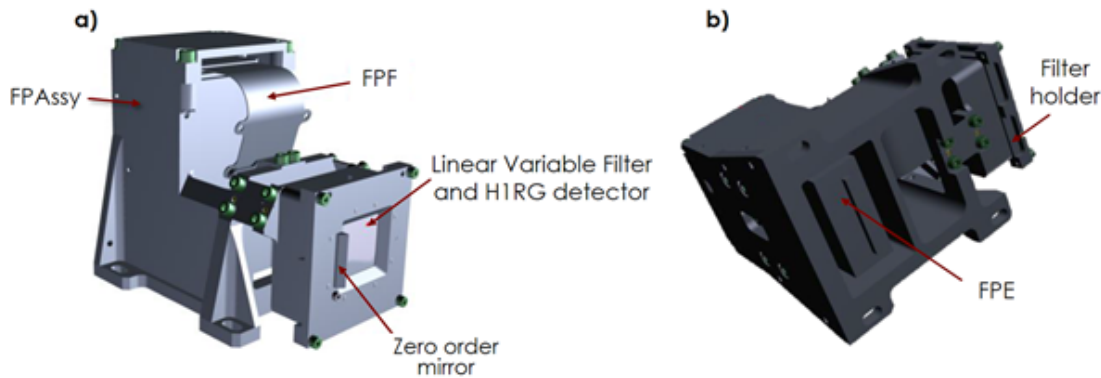


Figure 1. Components of the MAJIS VIS-NIR FPU: a) Frontal-top view, b) Rear-bottom view.²

MAJIS combines two different spectral channels: VIS-NIR ($0.5 \mu\text{m} - 2.35 \mu\text{m}$), and IR ($2.25 \mu\text{m} - 5.54 \mu\text{m}$)³. The MAJIS VIS-NIR detector needs to be characterized in the laboratory, before being tested at instrument level, to finally being integrated on the spacecraft⁴. In this way, it will be possible to verify and validate the performances of the detectors regarding the in-flight operation environment. The Royal Belgian Institute for Space Aeronomy (BIRA-IASB) and the Royal Observatory of Belgium (ROB) are in charge of the full characterization of the spare (SM) and flight models (FM) of the MAJIS VIS-NIR detectors⁵. A special instrument was developed at BIRA-IASB facilities in 2019 to prepare the characterization of the MAJIS VIS-NIR detectors⁶. However, before the delivery of the detectors, the facility was thermally and optically validated with the Structural Model (STM) and the Engineering Model (EM) of the VIS-NIR Focal Plane Unit (FPU)⁷.

The MAJIS VIS-NIR FPU (Figure 1), consists of the following items:

- Focal Plane Array (FPA): HgCdTe detector array of $1024 \times 1024 \text{ pix}^2$.⁸
- Linear Variable Filter (LVF): Optical cut-off high pass VIS-NIR filter.
- Focal Plane Electronics (FPE): SIDECAR/ASIC module.
- Focal Plane Flex (FPF): The flex cable interface between the FPA and the FPE.
- FPAssy: Thermo-mechanical housing of the FPU.
- FPE Optical Head (FPE-OH): Internal harness to link the FPE to the Proximity Electronics (PE).

The FPU guarantees the cleanliness of the internal components, the detector alignment, the nominal thermal conditions, the power and data connections with the PE, and it reduces the radiation emitted from its inner walls and other warm elements of the FPU. The FPU is provided with two temperature Cernox sensors to continuously monitor the temperature of the FPA and the FPE, and a survival line that includes three PT1000 temperature sensors and two heaters on the FPE. During the characterization campaigns of the MAJIS VIS-NIR detectors, the FPU can be thermalized within a temperature range from 116 K to 150 K inside a high-vacuum chamber. However during the characterization campaigns, neither the thermometry devices nor the heaters of the FPU are intended to be used for thermal control². Instead, the FPU is thermalized by an Oxygen-Free High Conductivity (OFHC) copper base plate that includes two PT100 calibrated temperature sensors and two heaters (for redundancy). Since the electrical harnesses of the FPE can dissipate up to 2 W of heating power, they are thermalized directly by the main thermal link of the FPU mount.

2. THERMAL-VACUUM SYSTEM AND SPECIFICATIONS

As part of the characterization facility at BIRA-IASB, a black anodized aluminum radiation shield (externally covered by MLI) harbors the FPU on the top of a special mount designed to thermalize the detector within its temperature range inside a high-vacuum chamber (Figure 2). The radiation shield allows the entrance of the light beam from its frontal panel through a baffle that limits the straylight outside the field of view of the detector. Thanks to a movable plate inside the radiation shield, three positions are offered in the radiation

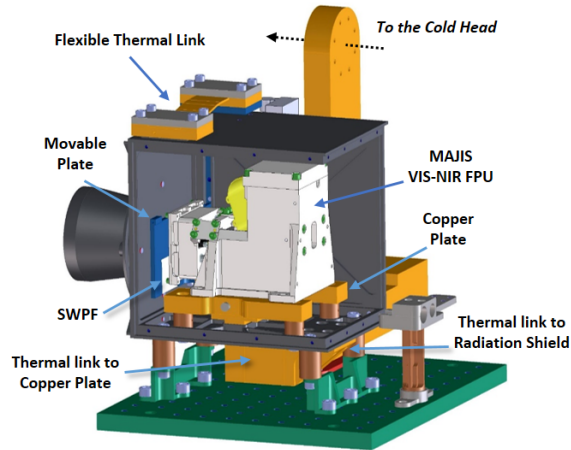


Figure 2. Diagram of the MAJIS VIS-NIR FPU inside the radiation shield of the thermo-mechanical mount of the characterization facility.⁶

shield: open, Short-Wave Pass Filter (SWPF) and close. The SWPF position removes background radiation from the CaF_2 viewport of the vacuum chamber and beyond. A typical threshold for negligible background radiation on the detector is set to $1 \text{ e}^-/\text{s}$. Therefore, the radiation shield and its movable plate must remain at a temperature below 172 K for the characterization temperature range⁹. The movable plate is thermalized by two flexible OFHC copper straps, one in contact with the external top surface of the radiation shield and another one with the copper base plate of the FPU mount inside the radiation shield. The thermalization of the FPU mount components is possible by using a closed cycle cryocooler¹⁰ that provides a cooling power of 60 W (at 77 K) with 25 K as the lowest accessible temperature without thermal load. The cold head of the cryocooler is thermally connected to the copper base plate of the FPU and the bottom part of the radiation shield by a rigid OFHC copper thermal link. Figure 3 shows the complete thermal lumped scheme of the FPU mount.

The minimum temperature that the FPU mount can achieve at the copper base plate level, is 95 K without thermal load⁶. Nevertheless, the thermal-vacuum facility guarantees that all components of the FPU mount, including the FPU itself, will work in safe conditions, summarized in Table 1. To reduce the possibility of molecular contamination on the FPU, the cryocooler is activated only when the vacuum level inside the vacuum chamber is below 1×10^{-4} mbar.

Several calibrated PT100 temperature sensors continuously monitor the FPU mount at the most critical

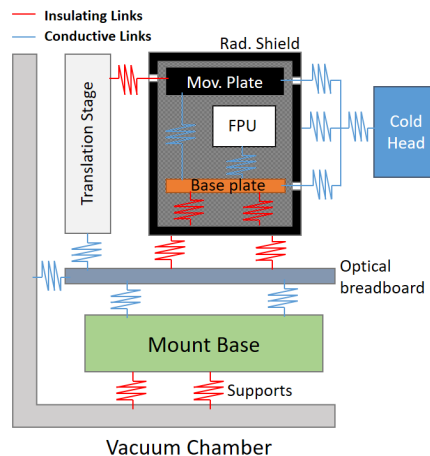


Figure 3. Thermal lumped scheme of the FPU mount.⁶

Table 1. Thermal-vacuum requirements for the security system of the VIS-NIR characterization facility.²

Parameter	Minimum value	Maximum value
FPA operative temperature	116 K	300 K
FPA non-operative temperature	110 K	323 K
FPE operative temperature	120 K	300 K
FPE non-operative temperature	120 K	323 K
Translation stage operative temperature	253 K	343 K
Vacuum level during measurements	N/A	10^{-5} mbar

locations: two in the copper base plate, two in the movable plate, one on the internal side of the radiation shield, one on the external side of the radiation shield, two on the main thermal link (close to the FPE harness and the copper base plate), two on the cold head of the cryocooler, one in the flexible thermal link of the movable plate, one on the baffle, and one on the motor of the translation stage. The temperature can be regulated at the copper base plate level (for FPA thermalization), the movable plate, the translation stage, and the cold head of the cryocooler. PID control loops provided by LakeShore monitors^{11,12} are used to this end. The LakeShore monitors are also used to activate alarms before the temperature overpasses the specified limits in the critical devices, with 5 K margin for the cold cases and 3 K margin for the hot cases. These margins were well characterized during the thermal validation of the facility with the MAJIS VIS-NIR STM detector⁷. National Instruments (NI) Data Acquisition (DAQ) modules are used to monitor the temperature of the survival line¹³ and the PT100 temperature sensors¹⁴ that are not monitored by the LakeShore monitors.

Similarly, the vacuum chamber status is continuously monitored by two pressure gauges, one with 30 % of accuracy between 1×10^{-9} and 1×10^3 mbar,¹⁵ and another one with 25 % and 50 % accuracy between 1×10^{-8} - 1×10^{-3} mbar and 1×10^{-3} - 1×10^3 mbar, respectively¹⁶. The corresponding controller of each pressure gauge¹⁷ provides two configurable relay outputs that can be activated above or below a specified vacuum level, which is useful for the detection of leaks or as indicators of the achievement of different vacuum regimes. The capacity of the vacuum chamber is 420 L. The high-vacuum level is achieved thanks to the combination of a dry primary pump in serial connection with a turbo-molecular pump. The primary pump¹⁸ has a pumping speed of 4 L/s and can achieve a vacuum level below 5×10^{-1} mbar in about 50 min. Around 25 min after the activation of the turbopump (260 L/s of pumping speed for N₂),¹⁹ the adequate vacuum level for the cryocooler is achieved in the chamber. It is intended that the pumping system is permanently active during the whole characterization campaign. The FPU mount was specially designed to counter the vibrations induced neither by the pumping system nor the cryocooler. The typical operating vacuum level inside the vacuum chamber is of the order of 10^{-7} mbar.

3. SECURITY SYSTEM DESCRIPTION

The security system mainly protects the VIS-NIR detector and its electronics in case of emergency, including temperature out of range and vacuum loss. A vacuum loss under cryogenic temperatures would be critical due to the risk of pollution and condensation on FPU surfaces. The security system is mainly constituted by a robust security rack, based on relays logic, that coordinates every device of the cryogenic system and heaters of the copper base plate, depending on the pressure and temperature conditions in the vacuum chamber and the functioning of the related equipment. Every switching function from the vacuum/temperature monitors in the facility, represents input signals for the security rack. In this way, the security rack will activate every device of the cryogenic system according to the vacuum and temperature conditions inside the chamber, to perform a complete cooling cycle of the mount from room conditions, either in manual or semi-automatic mode. Moreover, the security rack includes an emergency button that allows the user to interrupt the cryogenic system at any time, without compromising neither the safety of the detector nor the equipment. Figure 4 shows a schematic drawing of the cryogenic system and how it is linked to the security rack.

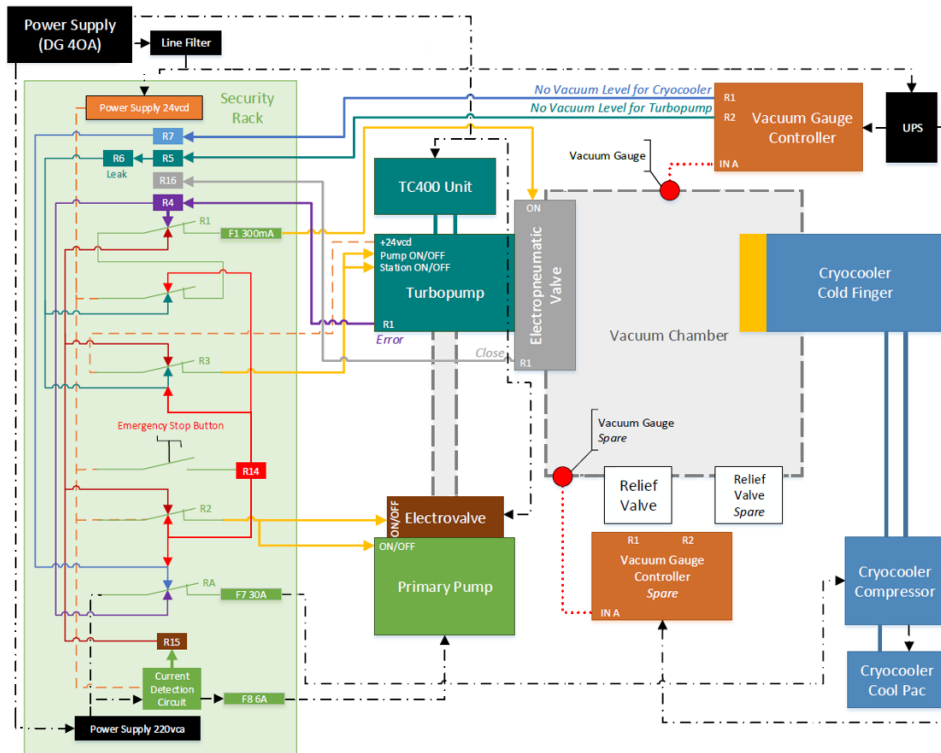


Figure 4. Cryogenic system of the VIS-NIR calibration facility managed by the security rack²⁰. The switching functions of the pressure monitors provide information about the vacuum level of the chamber to confirm the necessary conditions to allow the activation of the primary pump, turbopump and cryocooler. For security reasons, some of the elements are redundant. Although the user can manually activate or deactivate every equipment, the security rack reduces mistakes by conditioning the activation/deactivation of the equipment. The diagram shown does not represent the complete electrical circuit implemented in the security rack but provides enough information about the main safety actions it can perform.

As part of the security system, two normally-closed safety valves avoid abrupt vacuum loss due to failure of the pumping system or a power blackout. The main safety valve²¹ isolates the vacuum chamber from the pumping system with a closing time of 2 s. The secondary safety valve²² isolates the primary pump when it stops working (220 ms of closing time), which is possible by using a current detection circuit for the power supply of the primary pump. In consequence, the main valve can only be activated when the primary pump is in operation. Additionally, two pressure relief valves²³ (one redundant) open in case of overpressure during the venting procedure of the vacuum chamber. Both were individually calibrated to open at the minimum pressure difference (~ 0.1 bar) as a protection for the viewport of the vacuum chamber. Concerning the turbopump, it can only be activated when the vacuum level in the chamber is below 5×10^{-1} mbar and the primary pump is in operation. Similarly, the cryocooler can only be activated when the vacuum level in the chamber is below 1×10^{-4} mbar, and it is automatically deactivated if the pressure increases above 5×10^{-4} mbar or if the pumping system fails.

To avoid damage on the FPU due to temperature outside range, each LakeShore monitor is dedicated to protect one sensitive device in addition to its thermal regulation function. Every LakeShore monitor provides up to two alarm capabilities and two configurable switching functions that can be activated when the alarms are enabled (low and high temperature cases). The temperature difference of the FPA and the FPE with respect to the copper base plate is about 3 K (depending on the state of the movable plate) and 13 K, respectively for the coldest worst case (FPE OFF). Similar temperature differences can be considered for the hottest worst case (FPE ON). Therefore, the copper base plate also drives additional switching functions to protect the FPE, as a second security layer in case the FPE alarms do not work. In this way, when the temperature is too high

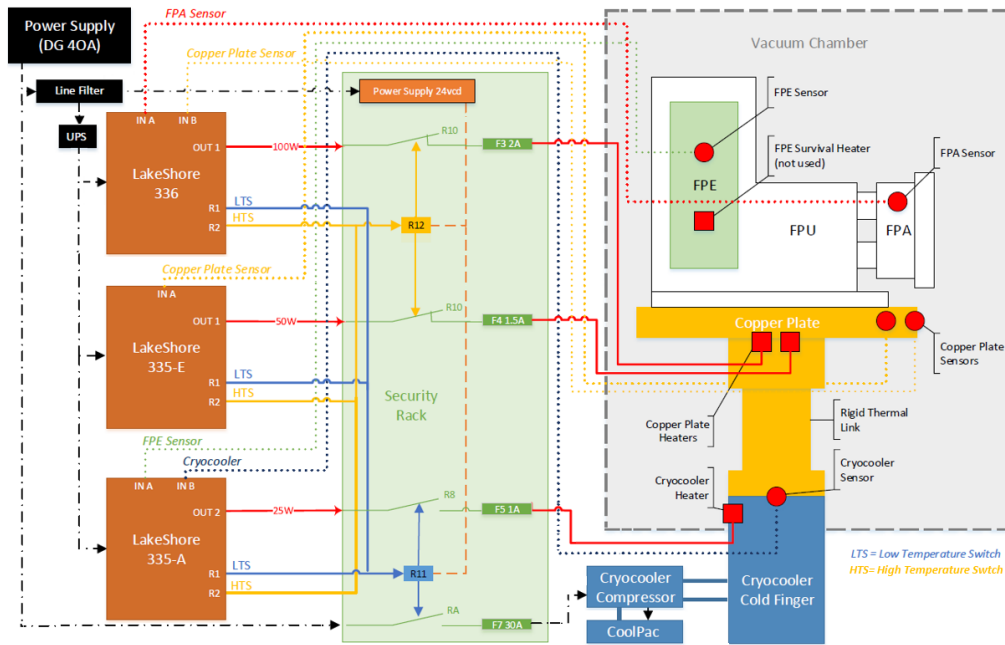


Figure 5. Temperature control system for the MAJIS VIS-NIR FPU managed by the security rack²⁰. The switching functions of the temperature monitors provide information about the temperature of the FPU to allow the functioning of the cryocooler and the heaters at the copper base plate. One redundant control loop is available in the copper base plate to thermalize the FPU. The translation stage can also drive the disconnection of the cryocooler, although it is not visible in this figure. The diagram does not represent the complete electrical circuit implemented in the security rack but provides enough information about the main safety actions it can perform.

(either on the FPA, FPE or copper plate), both thermal control loops on the copper plate are deactivated. In case the temperature is too low (either on the FPA, FPE or copper plate), the cryocooler is deactivated. The security rack prevents the reactivation of the disabled devices until the operating conditions are nominal again, although manual intervention is required. If one of the reference sensors for the temperature alarms fails, the low corresponding alarm will be automatically activated. Figure 5 shows a schematic drawing of the temperature control system and how it is related to the security rack.

The security rack is complemented by the Thermal Ground Support Equipment (TGSE) system, which provides a LabVIEW user-friendly interface to communicate in real-time the status of the detector and other components previously described, as well as the vacuum level inside the chamber. The TGSE displays and stores the temperature and pressure data monitored, and provides the possibility to configure the target temperatures to thermalize the FPU, activate and configure the different thermal control loops in the system, enable and configure the alarm values for each vacuum and temperature monitor, and remotely deactivate the cryocooler when considered necessary. When the TGSE is initialized at the beginning of the test, both thermal control loops in the copper plate are automatically activated at nominal temperature (FPA at 132 K), so during the cooling down process the FPA will stabilize at the specified setpoint minimizing the risk of achieving minimum temperatures in the facility and the possible activation of low temperature alarms. Because of the same philosophy, it is recommended to activate the thermal control loops corresponding to the translation stage and cryocooler. The TGSE is continuously verifying the correct functioning of the system, including the temperature and vacuum monitors, to immediately inform the user about any unexpected situation. To avoid user's mistakes, the TGSE limits the possible values for the FPU alarms and target temperatures outside the tolerance ranges. Additionally, it avoids the disconnection of the redundant thermal control loop of the copper base plate (unless the TGSE is operating in Test mode). Moreover, if a temperature alarm is activated by one of the LakeShore monitors, the other monitors will automatically activate their corresponding alarm for redundancy. In case the TGSE loses communication with a monitoring device, the monitor will keep its alarms and configurations, so

the system can continue operating nominally while the communication is reestablished. All messages and alerts provided by the TGSE are registered and sent to the users via SMS and email. Additionally, SMS and email alerts inform the user about an abrupt pressure change in the vacuum chamber (possible due to a leak or the closing of the electropneumatic valve), before it can be detected by the TGSE. The TGSE provides a webcam to visualize the state of the control panel of the security rack in real-time, that provides information about the state of the equipment conforming to the pumping and cryocooling system. It is worth mentioning that during the most critical tasks while operating the facility a trained operator is always present for fast reaction, in case an unexpected event takes place. Such tasks includes cooling-down, warming-up and target temperature changes.

The MAJIS VIS-NIR characterization facility disposes of two UPSes to supply for about 5 hours, the vacuum and temperature monitors, and the TGSE, Optical Ground Support Equipment (OGSE), and FPU-GSE computers. Therefore, the continuous monitoring and protection of the MAJIS FPU is possible even during power blackout events. In the course of a general power blackout, the BIRA-IASB electricity generator has the capability to supply the institute for about 24 hours during working days, or up to 48 hours during weekends. However, as soon as there is no power supply in any of the devices that constitute the pumping system, the main valve of the vacuum chamber automatically would close and the cryocooler and pumping system would stop working; although the temperature and vacuum conditions of the vacuum chamber could be followed by the TGSE.

4. SECURITY SYSTEM VALIDATION

The security system was fully validated in May 2020, before the delivery of the VIS-NIR FM detector²⁴. Figure 6 shows some pictures of the security rack, the TGSE and the vacuum system. The validation of the security system was divided in two phases: validation with simulated conditions and validation with real conditions (without FPU installed). Certainly before performing the validation of the security system, every device was individually tested, and a detailed Failure Mode Effects and Criticality Analysis (FMECA),²⁵ as well as a Fault Tree Analysis (FTA)²⁰ for the worst dreaded events, were made to evaluate the efficiency of the security system designed, following CNES and IAS requirements²⁶. Figure 7 shows the thermal-vacuum behavior of the facility during some of the tests performed during the validation of the security system. Note that the measurements corresponding to FPA and FPE come from additional temperature sensors installed on the copper base plate and not the real FPU components.

For the low temperature alarm tests, it was necessary to disable all thermal regulation loops on the FPU mount by setting the TGSE in Test Mode. In this way, the facility was forced to achieve a temperature below the defined temperature limits, with a rate of 0.7 K/min approximately. The alarms were tested individually to confirm their proper functioning by disabling the configured dependency induced by the TGSE, in which the activation of one alarm activates the others automatically for redundancy. About 4 minutes are necessary to confirm that

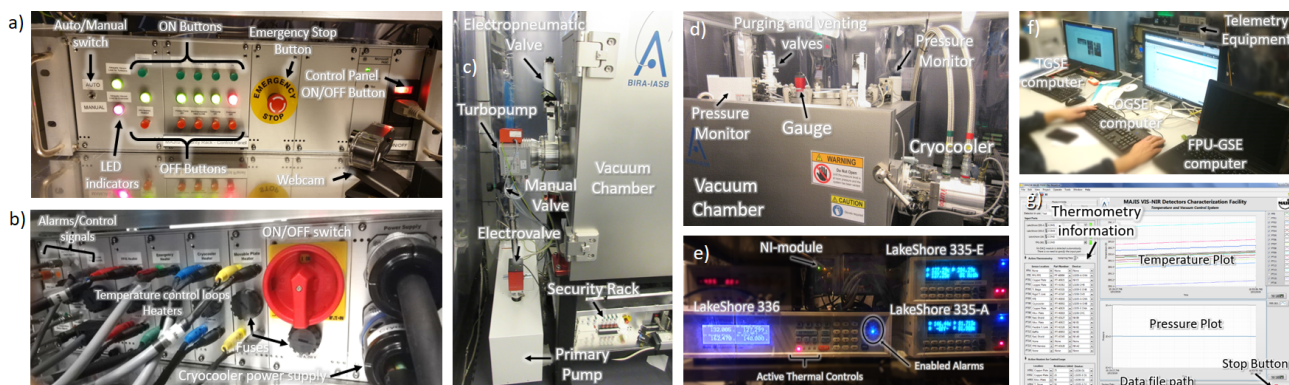


Figure 6. Security system components: a) Control panel of the security rack, b) rear panel of the security rack, c) pumping system, d) cryocooler and pressure gauge, e) temperature monitors and controllers, f) control room, g) TGSE user interface.

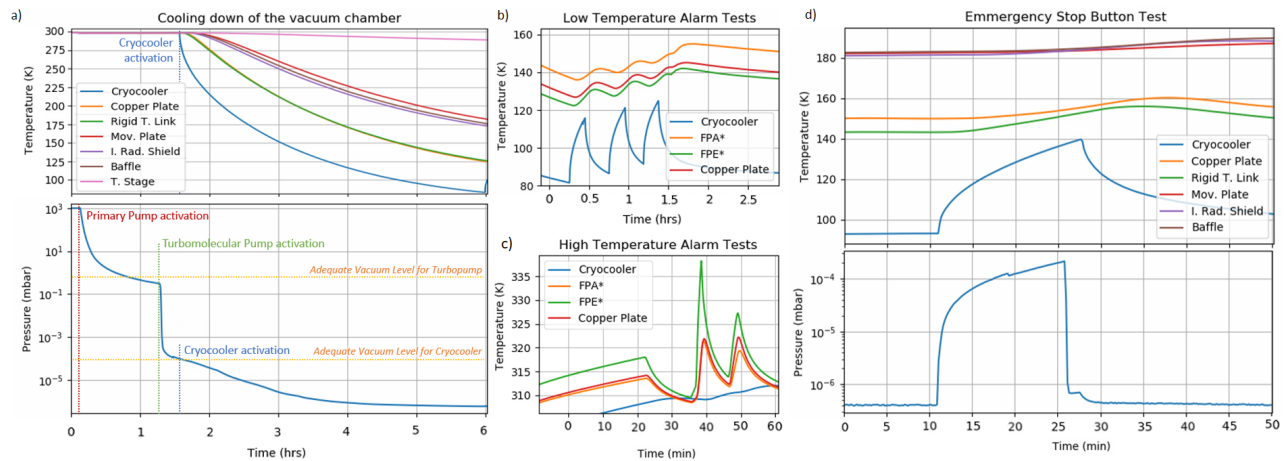


Figure 7. Validation tests of the security system²⁴. a) Thermal-vacuum performance of the chamber: a vacuum level below 5×10^{-1} mbar was achieved 50 min after the activation of the primary pump, and below 1×10^{-4} mbar 10 min after the manual activation of the turbopump; the cryocooler was automatically activated by the security rack. b) Low temperature alarm tests: the plot shows the continuous disconnection of the cryocooler due to the activation of the low temperature alarms of the FPE, FPA and Copper Plate, configured for this tests at 125 K, 141 K and 139 K, respectively; the reactivation of the cryocooler was manually performed in every case. c) High temperature alarm tests: the plot shows the continuous disconnection of both heaters of the copper plate due to the activation of the high temperature alarms of the FPE, FPA and Copper Plate, respectively, all configured for this tests at 318 K; note that the first slope corresponds to the expected temperature increase of the FPU during a real warm-up, the next ones were increased to accelerate the time of the test, the reactivation of the heaters was manually performed for every case. d) Emergency stop button test: the pumping system is disabled due to the closing of the electropneumatic valve that is reflected by the pressure increase of the chamber, similarly the temperature increase in the facility reflects the disconnection of the cryocooler; the temperature and pressure decrease are due to the successful reactivation of the pumping system and the cryocooler.

the temperature of the affected item is increasing after the disconnection of the cryocooler. The temperature of the copper plate increases up to 1 K more after the disconnection of the cryocooler and it recovers a safe temperature level around 5 minutes later. At this moment, the sound alarm from the corresponding LakeShore monitor stopped and it was possible to reactivate the cryocooler again.

Concerning the high temperature alarm tests, the thermal control loops of the copper plate were set to 320 K (maximum temperature allowed by the TGSE), with 318 K as the high temperature limits for the FPE, FPA and Copper Plate. Similarly to the low temperature case, the alarms were tested individually. By requirement, the FPU must not change its temperature by faster rates than 5 K/min.² Under nominal power, the temperature of the copper plate increases by 0.2 K/min. In order to accelerate the total time of this test, this rate was increased to 7.8 K/min when testing the high temperature alarms of the FPA and the Copper Plate. However the thermal behavior of the FPU with respect to the copper plate was characterized during the EM validation tests, and it was observed that even when the copper plate increases its temperature with a rate of 4.80 K/min, the FPA increases its temperature only by 0.51 K/min, and the FPE by 0.21 K/min, with a time delay of 1 and 3.5 minutes, respectively (Figure 8). In consequence, the FPU would not be exposed to such temperature changes during the characterization measurements. Taking as reference the FPE alarm test, the temperature of the copper plate decreased by 3.8 K/min after the deactivation of the thermal control loops. As expected, it was only possible to reactivate the control loops again when the temperature of the corresponding item (the copper plate, for this case) had decreased again below its defined high temperature limit. Both high and low temperature tests only reflect the thermal behavior of the copper plate.

The Emergency Stop Button test presented in this work, is representative for the other tests performed during the validation of the security system, such as the power blackout, leak detection, and failure of the pumping system. All these events produce the same main consequences in the facility: closing of both safety valves, and disconnection of the cryocooler. Note that after the closing of the main valve of the vacuum chamber (Figure

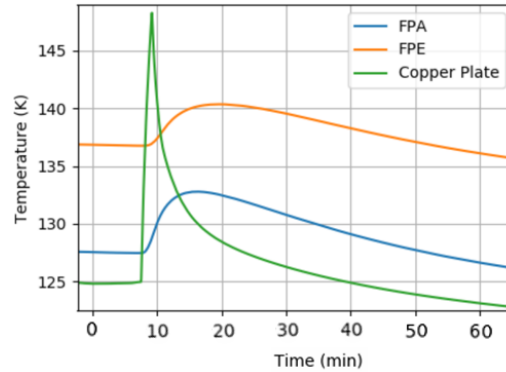


Figure 8. Thermal test performed during the validation tests of the facility with the MAJIS VIS-NIR EM FPU²⁷. The plot shows the thermal dependency between the components of the FPU and the copper plate. The FPE was inactive. In this test, the temperature of the copper plate increased its temperature with a rate of 4.80 K/min and about 1 minute later the temperature of the FPA increased with a rate of 0.51 K/min, followed by the FPE with a rate of 0.21 K/min, that started 3.5 minutes after the temperature change in the copper plate.

7) the high-vacuum level is lost by 2 orders of magnitude in about 2 minutes due to the deactivation of the pumping system. Later, the normal outgassing of the components that passively warm up after the deactivation of the cryocooler, slowly increase the pressure level of the chamber up to 10^{-4} mbar. If the pumping system had not been reactivated shortly after, the pressure would have increased up to 10^{-2} mbar in the following hours. Nevertheless even if that were the case, no contamination is expected in the FPU because once the chamber is under high-vacuum conditions again, the FPU would release again the molecules it could have trapped during the passive warm-up of the FPU mount. So during any kind of unexpected event at the facility, the FPU will remain safe under static vacuum conditions.

5. CONCLUSIONS

The VIS-NIR detectors characterization facility developed at BIRA-IASB, is able to safely thermalize the MAJIS/JUICE VIS-NIR detectors without compromising any of the elements of the FPU neither the facility itself during the characterization campaigns. It is worth mentioning that the thermalization is made at the base plate level of the detector and not directly by using its survival line, which is extremely avoided to guarantee that the heaters keep most of their lifetime hours. Usually a characterization campaign could last from one to six weeks, depending on the planning of measurements. Therefore it is critical that the security system guarantees the safety of the FM and SM detectors also during non-working hours.

The security system is mainly composed by a robust security rack based on relays-logic and the TGSE system. According to the current thermal-vacuum conditions of the detector and the vacuum chamber, the security rack reacts by disabling the closed cycle cryocooler (low temperature risk), the thermal heating system (high temperature risk), and the safety valves of the vacuum chamber (vacuum loss or over-pressure risk, accordingly). Additionally, it allows the semi-automatic remote control of the cryogenic system, mainly used to start the cooling-down cycle of the detector. The TGSE monitors the temperature and vacuum data from the corresponding monitoring devices and allows the user to configure the alarms values, the thermal control capabilities and when necessary, the remote disconnection of the cryocooler. The TGSE is complemented by an alert system to inform the user by SMS and email about any unexpected behavior of the facility at any time. The security system is also prepared in case of a power blackout event by immediately isolating the vacuum chamber from the pumping system, while the TGSE and monitoring devices (including thermal control) remain supplied by an UPS equipment. In case of an emergency, the security system also provides an Emergency Stop Button to properly deactivate the cryogenic system and isolate the vacuum chamber, so it can keep a static vacuum level without risk of contamination on the detector while dealing with the emergency.

Thanks to the inspection of CNES in October 2019, the previous security system developed for the characterization bench developed at BIRA-IASB, was significantly updated to mainly provide (at least) one additional

layer of security to every potential issue, a complete isolation of the vacuum chamber from the pumping system, and the impossibility to deactivate the thermal control system even during power blackout events²⁶. Moreover, the security system has now the capability to identify failures/errors from every device that constitutes the cryogenic system and aware the responsible operators asap. It is possible to highlight that in case of failure of the pumping system, the vacuum chamber is isolated from the primary pump in 220 ms, while the main valve of the chamber fully closes in 2 s. This represents a loss in vacuum level of 2 orders of magnitude, from nominal working conditions in the chamber. The pumps are configured to avoid autonomous venting. In the case of low temperature risk, the cryocooler is deactivated 5 K before achieving the minimum allowed temperature at the FPU, while the pumping system remains active to compensate the expected outgassing. At this case, the temperature of the copper base plate decreases by 1 K more before starting to increase its temperature again due to the disconnection of the cryocooler. Since the thermal response of the FPU is slower than the copper base plate, it is not expected that the temperature of the FPU components decrease by more than 1 K after the cryocooler disconnection. A similar behavior occurs during high temperature risk, although the alarms are set 3 K below the maximum allowed temperature at the FPU. The temperature alarms are driven by the temperature at the FPA, FPE and copper base plate. Moreover, now the temperature alarms are related between them, so when one alarm is activated, the additional corresponding ones are activated as well for redundancy.

The validation tests of the security system confirmed its correct functioning. During the validation tests, the activity of the facility was interrupted during different stages of a nominal operating state, including different vacuum regime. These tests were a tool to validate different procedures,^{28–30} including the procedures to properly identify and solve unexpected events,³¹ and the procedures to recover nominal conditions at the vacuum chamber without compromising any of the elements installed in the FPU mount,^{32,33} especially the MAJIS VIS-NIR FPU. In this way, the characterization facility was fully certified to receive and operate the MAJIS VIS-NIR FM and SM detectors at BIRA-IASB to proceed with their characterization.

Thanks to the versatility philosophy followed during the development of the calibration facility, the cryogenic and security systems can be easily adjusted to new cases, where different detectors can be safely characterized in the wavelength range of 0.4 μm - 2.65 μm at BIRA-IASB premises, especially flight models and when cryogenic conditions are needed.

ACKNOWLEDGMENTS

This project acknowledges funding by the Belgian Science Policy Office (BELSPO) by PRODEX-11 Project Proposal: *Characterization of JUICE/MAJIS VIS-NIR detectors* (PEA 4000124255), as well as by the Scientific Research Fund (FNRS) by the Aspirant Grant: 34828772 *MAJIS detectors and impact on science*. Additional funding is provided since end of 2019 by the ESA JUICE Project.

REFERENCES

- [1] Grasset, O., Dougherty, M., Coustenis, A., Bunce, E., Erd, C., Titov, D., Blanc, M., Coates, A., Drossart, P., Fletcher, L. N., et al., “Jupiter ICy moons Explorer (JUICE): An ESA mission to orbit Ganymede and to characterise the Jupiter system,” *Planetary and Space Science* **78**, 1–21 (2013).
- [2] MAJIS Team, “MAJIS FPU VIS-NIR Requirement Specifications,” tech. rep., Institute of Space Astrophysics (IAS) (2018). Ref: JUI-IAS-MAJ-RS-021.
- [3] Langevin, Y., Piccioni, G., and team, M., “MAJIS (Moons and Jupiter imaging spectrometer) for JUICE: objectives for the galilean satellites,” in [*European Planetary Science Congress*], **8**, 548–1 (2013).
- [4] Guiot, P., Vincendon, M., Carter, J., Lecomte, B., Poulet, F., Lami, P., and Langevin, Y., “JUICE/MAJIS on-ground calibration: challenges and setup design,” in [*Geophysical Research Abstracts*], **21** (2019).
- [5] Langevin, Y., Pascal, E., Renotte, E., Gérard, J.-C., Karatekin, Ö., and Ann-Carine, V., “Memorandum of Understanding between IAS and CSL, ULiège, ROB and BIRA-IASB.” 2015.
- [6] Bolsée, D., Van Laeken, L., Cisneros-González, M. E., Pereira, N., Depiesse, C., Jacobs, L., Vandaele, A. C., Ritter, B., Gissot, S., Karatekin, Ö., et al., “The characterization facility for the MAJIS/JUICE VIS-NIR FM and SM detectors,” in [*Space Telescopes and Instrumentation 2020: Optical, Infrared, and Millimeter Wave*], **submitted**, International Society for Optics and Photonics (2020).

- [7] Cisneros-González, M. E., Bolsée, D., Pereira, N., Jacobs, L., Van Laeken, L., Gérard, P., Cessateur, G., Robert, S., Vandaele, A., Karatekin, Ö., et al., “Validation tests of the calibration bench for the characterization of MAJIS/JUICE VIS-NIR detectors,” in [*M1T1 Upcoming and Future Planetary Missions and Instrumentation*], **13**, EPSC–DPS2019–551–1, EPSC-DPS Joint Meeting (2019).
- [8] Teledyne Imaging Sensors, *H1RGTM Visible and Infrared Focal Plane Array* (2018).
- [9] Van Laeken, L., *Development of experimental benches for radiometric characterization: Application to space instrument MAJIS VIS-NIR on JUICE.*, Master’s thesis, Université de Liège, Liège, Belgium (2019).
- [10] ARS Closed Cycle Cryocoolers, *Model CS104FT* (2010).
- [11] LakeShore, *Model 335 Temperature Controller* (2017).
- [12] LakeShore, *Model 336 Temperature Controller* (2017).
- [13] National Instruments, *NI-9219 Data Acquisition System for universal measurements* (2019).
- [14] National Instruments, *NI-9216 Data Acquisition System for PT100 RTD measurements* (2018).
- [15] Pfeiffer Vacuum, *PKR-361 Compact Full-Range Gauge* (2015).
- [16] Pfeiffer Vacuum, *MPT-200 Digital Pirani/Cold Cathode Gauge* (2015).
- [17] Pfeiffer Vacuum, *TPG-361 Single Gauge Channel Measurement and Control Unit for Active Line* (2015).
- [18] Pfeiffer Vacuum, *ACP 15, Standard, three phase, manual gas ballast* (2018).
- [19] Pfeiffer Vacuum, *HiPace 300 H Turbopump* (2018).
- [20] Cisneros-González, M. E., “Fault Tree Analysis (FTA),” tech. rep., Royal Belgian Institute for Space Aeronomy (BIRA-IASB) (2020). Ref: IASB-MAJ-FTA-2.2.
- [21] VAT, *High-Vacuum Gate Valve, series 12.1* (2018).
- [22] PfeifferVacuum, *Angle valve, electromagnetically activated. PF A44 506* (2011).
- [23] PfeifferVacuum, *120 VSU 016 Pressure relief valve* (2011).
- [24] Cisneros-González, M. E., “MAJIS VIS-NIR characterization bench design. Security system validation,” tech. rep., Royal Belgian Institute for Space Aeronomy (BIRA-IASB) (2020). Ref: IASB-MAJ-VR-001-2.0.
- [25] Cisneros-González, M. E., “Failure Mode Effects Analysis (FMECA),” tech. rep., Royal Belgian Institute for Space Aeronomy (BIRA-IASB) (2020). Ref: IASB-MAJ-FMECA-2.5.
- [26] Lazartigues, F., “CNES recommendations for Securing IASB test facility,” (2019). Ref: JUICE-MAJIS-RP-0351-CNES.
- [27] Bolsée, D., Van Laeken, L., Cisneros-González, M. E., Pereira, N., Ketchazo, C., and Haffoud, P., “VIS-NIR characterization bench. MAJIS VIS-NIR EM FPU validation campaign,” tech. rep., Royal Belgian Institute for Space Aeronomy (BIRA-IASB) (2020). Ref: IASB-MAJ-VR-004-0.7.
- [28] Cisneros-González, M. E., *Pumping and cooling down the vacuum system* (2020). Ref: IASB-MAJ-PRO-005-2.4.
- [29] Cisneros-González, M. E., *Turning off the pumping system* (2020). Ref: IASB-MAJ-PRO-008-2.2.
- [30] Cisneros-González, M. E. and Pereira, N., *Emergency procedure* (2020). Ref: IASB-MAJ-PRO-014-1.3.
- [31] Cisneros-González, M. E. and Depiesse, C., *Restore system after unexpected event* (2020). Ref: IASB-MAJ-PRO-017-2.0.
- [32] Depiesse, C. and Cisneros-González, M. E., *Recovering Cryogenic conditions* (2020). Ref: IASB-MAJ-PRO-018-2.1.
- [33] Cisneros-González, M. E., *How to restart the TGSE when needed* (2020). Ref: IASB-MAJ-PRO-020-1.2.

APPENDIX A. ACRONYMS

ASIC	Application-Specific Integrated Circuit
BELSPO	Belgian Science Policy Office
BIRA-IASB	Royal Belgian Institute for Space Aeronomy
CNES	National Centre for Space Studies
DAQ	Data Acquisition
EM	Engineering Model
ESA	European Space Agency
FM	Flight Model
FMECA	Failure Mode Effects and Criticality Analysis
FNRS	Scientific Research Fund
FPA	Focal Plane Array
FPE	Focal Plane Electronics
FPF	Focal Plane Flex
FPU	Focal Plane Unit
FTA	Fault Tree Analysis
GSE	Ground Support Equipment
HTS	High Temperature Switch
IAS	Institute of Space Astrophysics
IR	InfraRed wavelength range
JUICE	JUpiter Icy Moons Explorer
LTS	Low Temperature Switch
LVF	Linear Variable Filter
MAJIS	Moons And Jupiter Imaging Spectrometer
MLI	Multi-Layer Insulation
NI	National Instruments
NIR	Near-InfraRed wavelength range
OFHC	Oxygen-Free High Conductivity
OGSE	Optics Ground Support Equipment
OH	Optical Head
PE	Proximity Electronics
PID	Proportional-Integral-Derivative
ROB	Royal Observatory of Belgium
SIDECAR	System Image, Digitizing, Enhancing, Controlling, And Retrieving
SM	Spare Model
SMS	Short Message Service
STM	STructural Model
SWPF	Short-Wave Pass Filter
TGSE	Thermal Ground Support Equipment
UPS	Uninterruptible Power Supply
VIS	VISible wavelength range